13th World Conference on Earthquake Engineering
Vancouver, B.C., Canada
August 1-6, 2004
Paper No. 1997

DUCTILE DESIGN OF STEEL ROOF DECK DIAPHRAGMS FOR EARTHQUAKE RESISTANCE

C.A. ROGERS[1], R. TREMBLAY[2], W. YANG[3], E. MARTIN[4]

SUMMARY

The use of the steel roof deck diaphragm as the energy-dissipating element in the lateral load carrying path of single-storey steel buildings is investigated. A summary of the most recent experimental and analytical research is presented. This paper concentrates on the effect of non-structural components and the presence of end-lap joints on diaphragm performance. Large-scale diaphragm tests revealed that the presence of non-structural roofing components, such as gypsum and fibre board, caused the in-plane diaphragm stiffness and strength to increase by 49% and 24%, respectively. Furthermore, shorter length panels with end-lap connections resulted in an overall reduction in the diaphragm stiffness and strength because of a loss in warping rigidity. The results of non-linear time history dynamic building analyses, which accounted for the variation in behaviour due to the non-structural roof components and the use of end-laps, are also included. These analyses showed that the end-laps did not have a significant effect on the inelastic demand placed on the diaphragm, whereas the non-structural components caused a reduction in demand. Global ductility demand on the building was in the range of the R_d values used for design, while local ductility demand in the diaphragm was variable with the highest values near the inelastic shear distortion limit based on previous experimental results when $R_d = 3.0$ was used.

INTRODUCTION

Common to North America are single-storey steel buildings, which are often composed of the Gerber framing system with open web steel joists for the roof, HSS columns, concentrically braced frames along the perimeter walls and a steel roof deck diaphragm to transfer lateral wind and seismic loads to the bracing bents (Figure 1a). The recently introduced 2001 version of the CSA S16 Steel Structures Standard [1] requires that a capacity based design strategy be implemented for seismic design in Canada, where the brace elements in the seismic force resisting system (SFRS) are selected to carry the National Building

[1] Assistant Professor, Department of Civil Engineering and Applied Mechanics, McGill University, Montreal, QC, Canada
[2] Professor, Department of Civil, Geological and Mining Engineering, École Polytechnique, Montreal, QC, Canada
[3] Postgraduate Student, Department of Civil, Geological and Mining Engineering, École Polytechnique, Montreal, QC, Canada
[4] Engineer, Martoni, Cyr & Associates Inc., Montreal, QC, Canada

Code [2] lateral loads. All other elements in the SFRS, such as the brace connections, columns, anchor rods, foundations, roof diaphragm, etc, must be designed to resist forces associated with the actual capacity of the braces (Figure 1b). It is possible that other design requirements may control the sizing of braces, such as the limited number of member sizes that are available and limits on overall slenderness and element flat width ratios, which exist to control failure caused by low cycle induced fatigue. All other elements in the SFRS must be chosen such that their capacity is higher than that of the oversized braces. This can lead to much larger column sections, foundations, connections, as well as thicker roof deck panels and diaphragms with more connections. An alternative approach is for the engineer to select the roof deck diaphragm as the fuse element in the SFRS (Figure 1c). In this case the sheet steel panels and the connections that make up the diaphragm would be expected to enter into the inelastic range of behaviour in order to dissipate the energy developed in the structural system during a seismic event (Figure 1d).

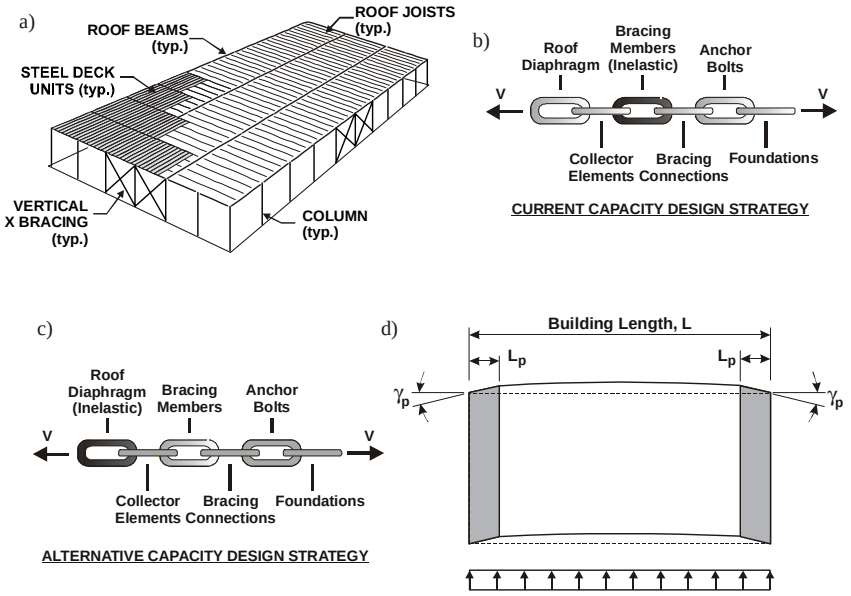

Figure 1 : Single-storey steel buildings: a) Typical building; b) Strong diaphragm design approach; c) Weak diaphragm design approach; d) Zones of inelastic deformations in diaphragms

Current diaphragm design methods, e.g. the Steel Deck Institute (SDI) [3,4] and the Stressed Skin [5] design approaches, were formulated mainly from the results of monotonic testing of single sheet length bare steel roof deck diaphragms. Information on the inelastic behaviour of roof deck diaphragms was needed to develop an alternative seismic design method for both the diaphragm and the overall structure of the building; hence a research program was initiated at Ecole Polytechnique of Montreal in 1999. Initial laboratory testing and analytical studies showed that roof deck diaphragms with appropriate fastener detailing can be used as the energy dissipating fuse element in the SFRS [6,7,8,9]. In this past research the results of non-linear dynamic analyses of four representative buildings, using a suite of earthquake ground motions for the east and west of North America, were first used to quantify the typical demand placed on the roof diaphragm and to develop appropriate loading protocols for testing. Tests on cantilever diaphragm specimens made of 0.76 and 0.91 mm thick corrugated steel deck panels showed that variables having an effect on the performance of the diaphragm system included; configuration of the sheet steel panels, the type and spacing of the fasteners, and the applied loading history. Diaphragms constructed with screwed side-lap fasteners and nailed deck-to-frame connectors were able to sustain large inelastic deformation cycles with limited strength degradation and could be relied on to resist seismic effects in the inelastic range.

This paper reports on two additional aspects of this research program: 1) The effect of non-structural components on diaphragm behaviour, and 2) the influence of end-laps and short panel lengths on inelastic diaphragm performance. It was initially anticipated that roofing and end-laps (sheet length) would affect the stiffness and strength of the diaphragm, resulting in a period change of the building vibration and thereby influencing the seismic response of single-storey steel buildings. Given this assumption, large-scale diaphragm tests were completed on specimens with non-structural roofing components as well as with end-laps and short sheet lengths. Additional non-linear time history analyses were also carried out on a representative building for which the roof deck elements were given inelastic properties that matched the diaphragm behaviour observed during testing.

DIAPHRAGM TEST PROGRAM

A cantilever, 3.6 × 6.1 m load frame with pinned corner connections was used to perform monotonic, short duration seismic and cyclic diaphragm tests (Figure 2). The large-scale test specimens represent a portion of the overall roof diaphragm in a typical single-storey structure. The overall test program has included to-date a total of 46 diaphragm tests, with the properties as well as the measured peak shear strength, S_u, and shear stiffness, G', of a selection of specimens provided in Table 1. The specimen number in the table includes the depth of the deck (mm), the thickness of the deck (mm × 100), the length of the sheet (m), the fastener type (e.g. NS for Nail-Screw), the type of loading (e.g. M for Monotonic), and a sequential number. For simplicity, only the sequential numbers are used in the text. Tests 1 and 4 were performed by Essa et al. [7], tests 19 to 37 by Martin [8] and tests 38 to 46 by Yang [9]. This paper documents the results of a series of tests and an analytical study carried out by Yang.

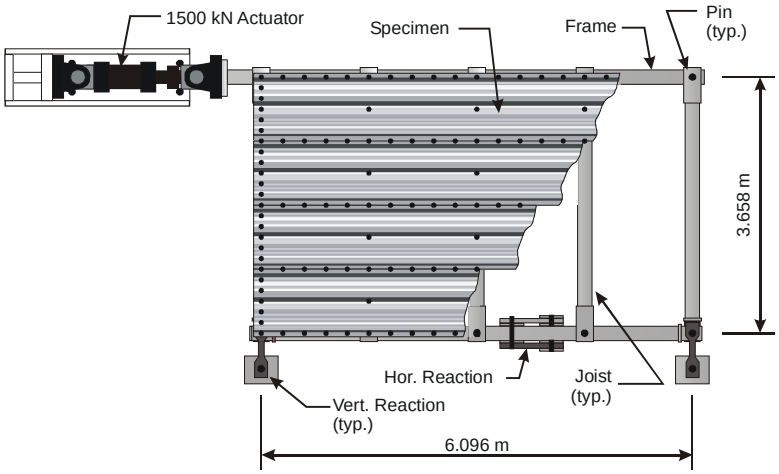

Figure 2 : Diaphragm test set-up (schematic plan view).

Specimens 39 through 42 were constructed of three full-width and two half-width 0.76 mm thick half-length panels (3.048 m) in order to evaluate the effect of end-lap connections (located along line 11 Figure 3a) and panel length on the shear properties. Five panels over the width of the diaphragm were specified to reduce the boundary condition effect along the 6.1 m sides of the test frame due to the relative difference in strength and stiffness between the edge frame fasteners (along lines A and M Figure 3a) and the interior side-lap fasteners (along lines D, G and J Figure 3a). The panels were connected to one another, to the perimeter frame members, as well as to the joist beams. Two different combinations of side-lap and frame connectors were studied: No. 12 Hilti self-drilling screws with Hilti X-EDNK22-THQ12 nails (S-N design) (Figure 3e), and button punched side-laps with standard welded (no washers) frame connections (BP-W design) (Figure 3d). Specimens 43 to 46 consisted of three full-width and two

half-width 0.76 mm thick full-length panels (6.1 m) connected with No. 12 Hilti self-drilling screws with Hilti X-EDNK22-THQ12 nails (S-N design) (Figure 3e). Non-structural roofing components were also installed in tests 45 and 46, on top of the bare steel roof deck panels. For all specimens tested by Yang, the spacing of the fasteners was 305 mm in both directions, i.e. at every other flute in the direction perpendicular to the loading. Tests 43 and 44 were composed of five full-length panels such that a comparison could be made with specimens 39 and 40 in terms of the influence of the end-laps.

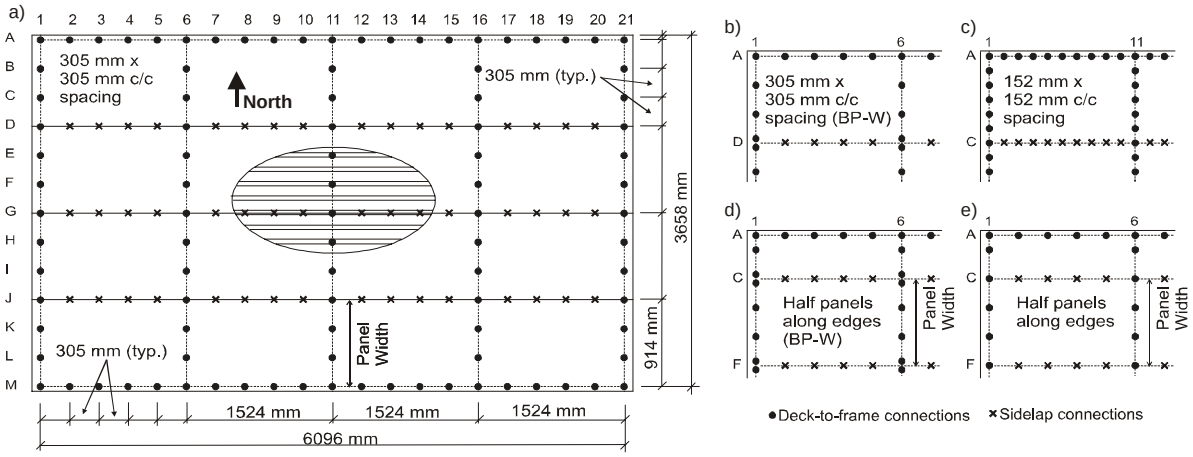

Figure 3 : Layout of deck-to-frame and side-lap connections (plan view).

Specimens with Non-Structural Roofing Components

The choice of a roofing system was based on a literature review and on advice received from the Association des Maîtres Couvreurs du Québec, the Ontario Industrial Roofing Contractors Association, as well as from various roofing contractors. The roofing composition known as SBS-34 was used for the large-scale cantilever diaphragm tests 45 and 46. This conventional adhered roof system, commonly used in Canada, is composed of the following layers (from top to bottom) (Figures 4 & 5):

i) Two layers (4 mm + 2.2 mm) of synthetic rubber SBS (Styrene-Butadiene-Styrene) waterproof membrane;
ii) One layer of 25.4 mm thick flame resistant wood fibre board, hot bitumen adhered;
iii) One layer of 63.5 mm thick polyisocyanurate (ISO) insulation, hot bitumen adhered;
iv) Two layers of paper vapour retarder (No. 15 asphalt felt), hot bitumen adhered;
v) One layer of 12.7 mm thick gypsum board, 12 screws per 2.4×1.2 m panel mechanically fastened.
vi) 0.76 mm Canam P3615B ASTM A653 [10] steel deck.

Figure 4 : Section view of diaphragm specimen showing non-structural components and steel deck

Table 1 : Diaphragm test specimens

Test	*Side-lap*	*Frame*	*Deck Profile*	*Loading Protocol*	S_u (kN/m)	G' [11] (kN/mm)
38-76-6-WB-M-1[*]	button punch	weld [2]	P3615 0.76 mm	M	8.05	2.14
38-76-6-NS-M-4[*]	screw	nail (H) [1]	P3615B 0.76 mm	M	12.3	3.12
38-91-6-NS-M-19	screw	nail (H) [1]	P3615B 0.91 mm	M	16.7	4.13
38-76-6-WB-SD-20	button punch	weld [2]	P3615 0.76 mm	SD	9.81	2.44
38-91-6-WB-SD-21	button punch	weld [2]	P3615 0.91 mm	SD	13.8	3.16
38-91-6-W'W-M-22	weld+washer[3]	weld+washer[4]	P3615B 0.91 mm	M	32.1	4.54
38-91-6-W'W-SD-23	weld+washer[3]	weld+washer[4]	P3615B 0.91 mm	SD	34.6	4.60
38-91-6-W'W-LD-24	weld+washer[3]	weld+washer[4]	P3615B 0.91 mm	LD	33.2	4.36
38-91-6-NW-M-25	weld+washer[3]	nail (H) [5]	P3615B 0.91 mm	M	22.5	4.33
38-91-6-NW-SD-26	weld+washer[3]	nail (H) [5]	P3615B 0.91 mm	SD	26.5	4.09
38-91-6-NW-LD-27	weld+washer[3]	nail (H) [5]	P3615B 0.91 mm	LD	26.2	3.64
38-76-6-NS-SD-28	screw	nail (H) [1]	P3615B 0.76 mm	SD	14.1	2.45
38-76-6-NS-LD-29	screw	nail (H) [1]	P3615B 0.76 mm	LD	13.6	2.39
38-76-6-NS-M-30[6]	screw	nail (H) [1]	P3615B 0.76 mm	M	23.4	13.5
38-76-6-NS-SD-31[6]	screw	nail (H) [1]	P3615B 0.76 mm	SD	26.5	15.0
38-91-6-NS-M-32[6]	screw	nail (H) [1]	P3615B 0.91 mm	M	34.4	18.3
38-91-6-NS-SD-33[6]	screw	nail (H) [1]	P3615B 0.91 mm	SD	35.2	18.4
38-91-6-NS-SD-34	screw	nail (H) [1]	P3615B 0.91 mm	SD	17.0	4.01
38-91-6-NS-LD-35	screw	nail (H) [1]	P3615B 0.91 mm	LD	17.3	3.90
38-76-6-WB-SD-36	button punch	weld [2]	P3615 0.76 mm	C+SD[7]	5.80	2.40
38-91-6-WB-M-37	button punch	weld [2]	P3615 0.91 mm	M	12.6	3.32
38-91-6-NS-SD-38	screw	nail (B) [8]	P3615B 0.91 mm	SD	15.2	3.52
38-76-3-NS-M-39[9,10]	screw	nail (H) [1]	P3615B 0.76 mm	M	11.3	1.73
38-76-3-NS-SD-40[9,10]	screw	nail (H) [1]	P3615B 0.76 mm	SD	12.7	1.58
38-76-3-WB-M-41[9,10]	button punch	weld [2]	P3615 0.76 mm	M	9.14	1.65
38-76-3-WB-SD-42[9,10]	button punch	weld [2]	P3615 0.76 mm	SD	10.3	1.54
38-76-6-NS-M-43[10]	screw	nail (H) [1]	P3615B 0.76 mm	M	13.4	2.58
38-76-6-NS-C-44[10]	screw	nail (H) [1]	P3615B 0.76 mm	C+M[13]	10.9	2.85
38-76-6-NS-M-R-45[10,12]	screw	nail (H) [1]	P3615B 0.76 mm	M	15.6	4.17
38-76-6-NS-C-R-46[10,12]	screw	nail (H) [1]	P3615B 0.76 mm	C+M[13]	15.9	3.90

[1] Hilti (H) X-EDNK22-THQ12 fastener for nailed frame connections and 12-14×7/8" fastener for screwed side-lap connections.

[2] Welded frame connections were made with 16 mm diameter arc spot welds.

[3] Welded side-lap connections with washers.

[4] Welded frame connections with washers.

[5] Used Hilti (H) X-EDNK22-THQ12 fastener for nailed frame connections.

[6] All fasteners spaced at 152 mm o/c in both directions, spacing in all other tests equal to 305 mm.

[7] 200 cycles at 0.4 γ_u and 2 cycles at 0.6 γ_u prior to short duration loading protocol.

[8] Buildex BX14 fastener for nailed frame connections and 12-14×7/8" fastener for screwed side-lap connections.

[9] Deck sheets are 3.048 m long with an end lap connection at the specimen midpoint.

[10] Specimens are made of 5 deck sheets (3 full width and 2 half width at N and S edges).

[11] Secant shear stiffness based on 0.4 S_u.

[12] Specimen composed of steel deck and non-structural roofing components

[13] Repeated cycles at 0.2, 0.4 and 0.6 P_u prior to monotonic protocol

[M] Monotonic. [SD] Short Duration. [LD] Long Duration. [C] Cyclic.

[*] Tests BP-W (1) and S-N (4) carried out by Essa *et al.* [7].

Figure 5 : View of diaphragm specimen with roofing material (Test 45)

Short Duration Seismic Loading Protocol

Prior to the testing carried out by Yang [9] an analytical study was completed by Martin [8] to assess the demand to be imposed on the cantilever diaphragm test specimens. This study involved four different buildings (Figure 1a) with dimensions of: 15 × 30 × 5.4 m, 30 × 60 × 6.6 m, and 60 × 120 × 9.0 m. The fourth building was similar, yet measured 30 × 120 × 6.6 m and had an additional bracing line at mid-length acting in the direction parallel to the short walls. The most ductile combination of fasteners found by Essa et al. [7], i.e. screwed side-laps and nailed deck-to-frame connectors, was assumed for the design of all diaphragms. The structures were designed to meet the most recent CSA S16 Steel Standard [1] and the proposed 2005 National Building Code [2]. The National Building Code allows for reduced seismic forces in design, that is $V = V_{elastic} / R_d R_o$. Two trial values of R_d were chosen for the seismic design: 2.0 and 3.0, and in both cases an overstrength factor, $R_o = 1/\phi = 1/0.6 = 1.67$ was used, based on a resistance factor for mechanically connected diaphragms. Further information on these force modification factors can be found in Mitchell et al. [11]. Two Canadian sites were selected, each with a relatively high seismic risk: Victoria, British Columbia, situated on Vancouver Island which is along the Pacific Northwest Coast and Quebec City, Quebec, on the St. Lawrence River, in eastern Canada. The behaviour of the buildings was examined in the direction parallel to the short walls because of the greater shear flow demand on the diaphragm in that orientation.

Nonlinear dynamic analyses of the structures were carried out using the RUAUMOKO computer program [12] with the roof diaphragm modeled as a deep horizontal plane truss (Figure 6). A Stewart hysteretic model [13] was selected for the diagonal roof truss members in order to reproduce the cyclic inelastic response measured by Essa et al. [7] for the screw-nail diaphragm system. Based on quasi-static reversed cyclic tests, Essa et al. recommended that the plastic shear deformation of screw-nail diaphragms be limited to 10×10^{-3} radians. Beyond this deformation, the strength of the diaphragm was found to degrade below 80% of the peak load. A tension-only bi-linear with slackness hysteretic model with zero buckling strength was adopted for the vertical bracing members because it best represented the behaviour of a flat plate brace element. The building models were subjected to a suite of earthquake ground motions from the east and west of North America. Information obtained on the inelastic response of the roof diaphragm from the results of the analyses was evaluated and used to develop the short duration (SD) loading protocol (Figure 7). The large inelastic deformation cycles were arranged in an increasing order and combined with the smaller amplitude cycles so that the unique SD loading signal could be used to study the performance of a single test specimen under three different conditions: eastern Canada for $R_d = 3.0$

(first 14.5 cycles), western Canada for R_d = 2.0 (first 30.5 cycles), and western Canada for R_d = 3.0 (total of 44 cycles). The frequency of oscillation was set equal to 2.0 Hz for the small and intermediate amplitude cycles and to 1.0 Hz for the large cycles. For a given diaphragm specimen, the amplitudes of the test loading cycles were established based on the results of a matching monotonic test. A more detailed discussion of the development of the short duration loading protocol can be found in Martin [8] and Tremblay et al. [6].

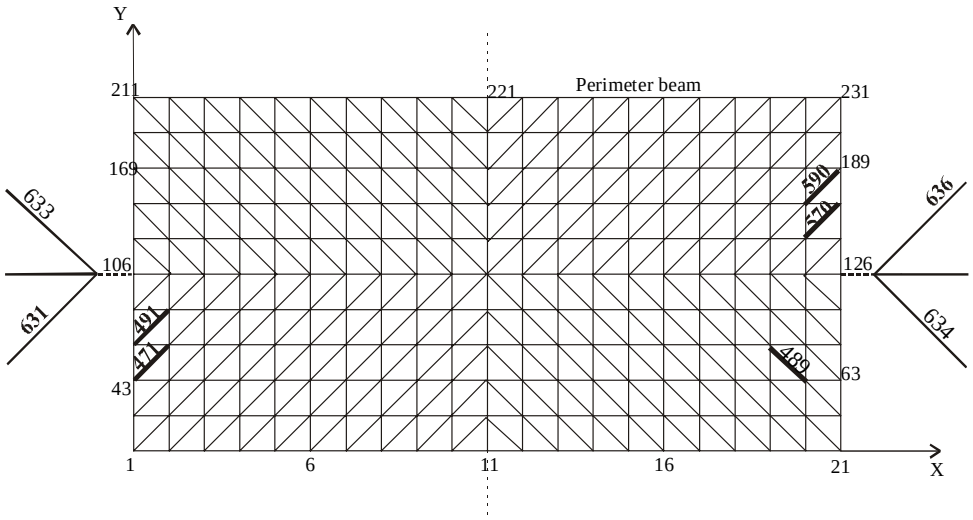

Figure 6 : RUAUMOKO 2D building model

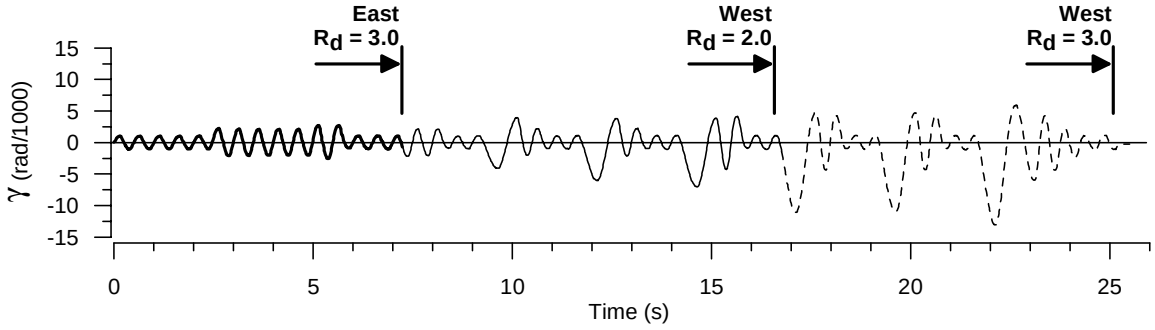

Figure 7 : Short Duration (SD) seismic loading protocol

BEHAVIOUR OF DIAPHRAGMS AND COMPARISON OF TEST RESULTS

Monotonic Tests

A graph showing the shear force vs. shear rotation of a selection of screw-nail and button punch-weld monotonic test specimens (39, 41, 43 & 45) is provided in Figure 8. A comparison of the effect of end-laps, and indirectly the influence of sheet length, on the shear stiffness and strength was possible through the testing of specimens 39 and 41. The use of the shorter sheet length resulted in a greater degree of cross-section warping deformation (Figure 9), which significantly reduced the measured shear stiffness from 2.58 kN/mm (Test 43) to 1.73 kN/mm (Test 39) (Table 1). Tests 43 and 39 were similarly constructed specimens, with the only difference being the end-lap and sheet length. The shear strength of the end-lap specimen was lowered by 15% due again to the increased warping of the panel.

The non-structural roofing components provided a significant increase in the shear strength (24%) measured for the large-scale diaphragm specimens (Figure 8 Test 45). During the loading process the gypsum board, which is quite rigid in its plane and also possesses a flexural stiffness, greatly restrained the warping of the panels (Figure 10). This warping restraint directly increased the shear stiffness, and indirectly reduced the stress in the fasteners, and thus helped to increase the strength of the diaphragm specimen. The increase in shear stiffness was even more significant (49%), once again due to the diminished warping of the panel cross-section.

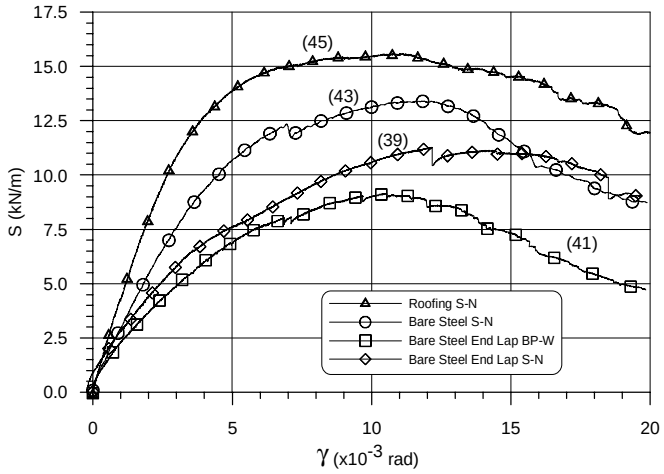

Figure 8 : Monotonic test results for 0.76 mm deck specimens

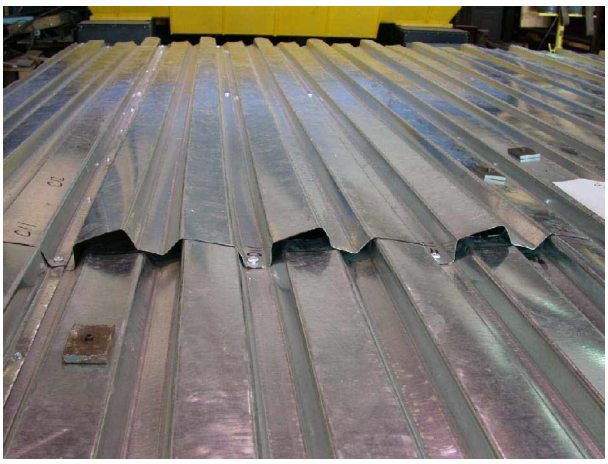

Figure 9 : Warping of profile at overlap panel end (Test 39)

Figure 10 : Warping deformation of steel deck restrained by non-structural components (Test 45)

Short Duration Seismic Tests

The shear force vs. shear rotation hysteresis of three comparable tests (28, 40 & 42) is provided in Figure 11. Considering the two nail-screw connected specimens, the effect of the end-lap was to slim the hysteresis, which indicates that extensive plastic and non-linear deformations of the diaphragm did not take place. In addition, even after the short duration protocol had been run twice on Test 40, most of the connectors (nails & screws) had not been damaged. Furthermore, the shear stiffness of the end-lap specimen was measurably lower than the full panel length test (2.45 kN/mm vs 1.58 kN/mm). The shear deformation of specimen 40 was mostly limited to the elastic warping of the panel profile instead of permanent sheet damage at the connection locations. Similar to the monotonic tests, the shear capacity of the SD end-lap specimen (Test 40) was reduced by 10% in comparison with the full length specimen (Test 28).

The behaviour observed for the button punch – weld diaphragm (Test 42) was different than that recorded for Test 40, in that although warping of the panels was substantial a number of weld connections failed. This gave rise to the decreased capacity of the test specimen in the later cycles of the short duration protocol. The inability to maintain a shear resistance with increasing deformation, even though the panels were able to more easily warp and reduce the demand on the connections, indicates that the BP-W configuration is not adequate for inelastic seismic design.

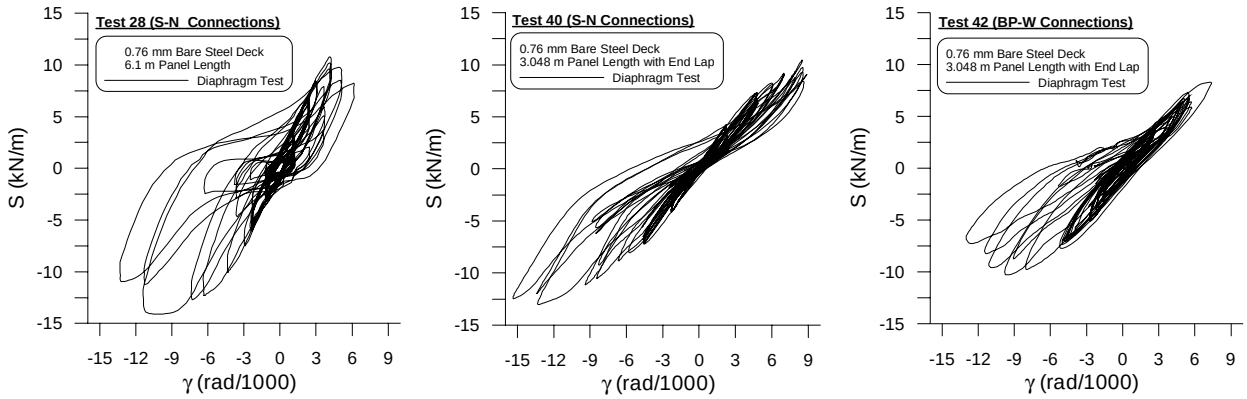

Figure 11 : Comparison of SD test results for 0.76 mm deck specimens

ANALYTICAL STUDY

The results of tests by Yang [9] were used to revisit the initial analytical study by Martin [8]. Martin showed that the nail-screw diaphragm design was the most promising in terms of inelastic behaviour and that $R_d = 2.0$ would be appropriate for design, however only buildings with type 1 (bare steel roof) diaphragms were considered. In this second analytical study the objectives were to improve the hysteretic diaphragm models based on the observed experimental response and to assess the effect of non-structural components and end-lap joints on inelastic diaphragm/building response. The $30 \times 60 \times 6.6$ m medium sized single-storey steel building, with a horizontal bracing bent length of $D_s = 7.5$ m, located in Victoria, BC was designed as described earlier. The analyses involved three different roof type scenarios as documented in Table 2.

For the three cases a nail-screw connected steel roof deck diaphragm was specified and designed to be the weak link in the SFRS. The same R_d values (2.0 and 3.0) as in the previous study were considered, along with $R_o = 1.67$. A study of the performance of this building when subjected to three different earthquake records (Figure 12), which were anticipated to cause the most significant inelastic deformation of the roof diaphragm based on the findings of Martin [8], was completed. The analysis time duration was chosen as 25 sec and the ground motions were scaled to match the 2005 NBCC design spectra over the applicable period ranges. The main difference between the previous analytical study by Martin [8] was that the Stewart hysteretic model was

improved in terms of a comparison with test results, and was modified to account for short duration loading, end-laps (short panels) and non-structural components, i.e. the hysteresis was based on the results of previous large-scale diaphragm tests, both SD and monotonic.

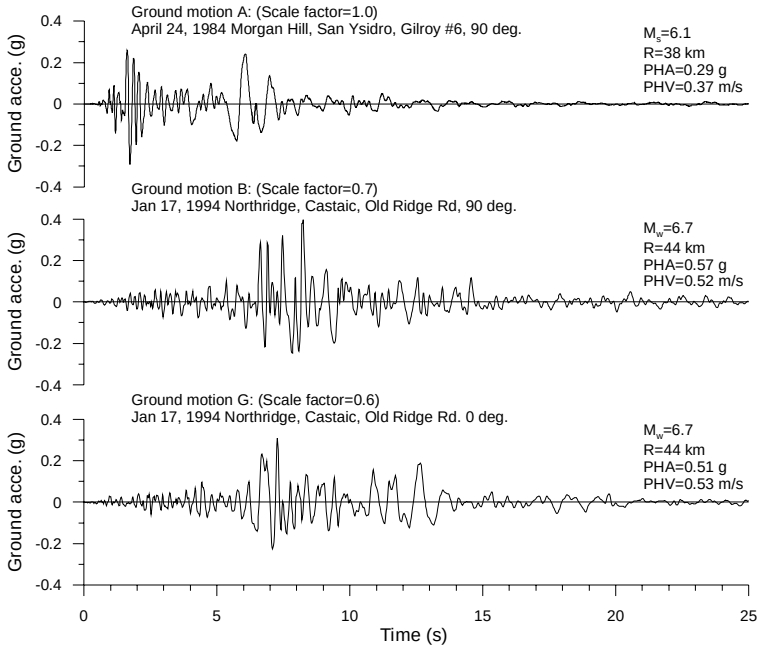

Figure 12 : Time history of selected ground motions

Table 2 : Roof type characteristics used for design

	Roof Type	*Panel Length*	*R_d = 3.0*			*R_d = 2.0*			*Tests*
			G' Design (kN/mm)	*S_u Design (kN/m)*	*Period (sec.)*	*G' Design (kN/mm)*	*S_u Design (kN/m)*	*Period (sec.)*	
1	Bare sheet	7500	11.9	10.1	0.69	4.57	15.3	0.80	28,31,33, 34 & 38
2[b]	Bare sheet	5625[b]	4.31	10.1	0.85	4.70	15.4	0.77	39 & 40
3	Roofing	7500	11.9[a]	10.1[a]	0.65	4.57[a]	15.3[a]	0.72	45 & 46

[a] For analysis purposes G' and S_u are increased to G' = 13.4 kN/mm and S_u = 11.9 kN/m for R_d = 3.0 and G' = 6.07 kN/mm and S_u = 17.1 kN/m for R_d = 2.0 due to the non-structural components.

[b] For roof type 2 the panel length was shortened to increase the end-lap effect.

The diaphragm design followed the SDI method [4] for bare steel deck. In order to calculate the strength and stiffness of roof type 3 for analysis purposes, values were added to the bare steel amounts based on test results. That is S_u and G' were equal to the SDI [4] based values determined for roof type 1, plus the estimated contribution of the non-structural components, i.e. the difference between test 28 and test 46, as follows:

$$S_{u,type3} = S_{u,type1} + (S_{u,test46} - S_{u,test28}) \quad (1)$$

$$G'_{type3} = G'_{type1} + (G'_{test46} - G'_{test28}) \quad (2)$$

The building designed with the type 2 roof had shorter deck panel lengths to increase the end-lap effect, which should have led to a decrease in diaphragm stiffness, e.g. 11.9 to 4.31 kN/mm for R_d = 3.0. However, for the R_d = 2.0 building this change in panel length necessitated an increase in the thickness of the profile from 0.76

to 0.91 mm to meet the strength requirements, which also affected the shear stiffness value. As such, the reduction in sheet length had no significant impact on the diaphragm properties for the $R_d = 2.0$ building.

A Newmark constant average acceleration method was used in the time history analysis with a time step of 0.001 sec. Rayleigh or a proportional damping model was used with a critical damping ratio of 5% for the first two modes of vibration. A two-dimension analysis model was used to simulate the real 3D structure (Figure 6), in a similar fashion as successfully implemented by Martin [8]. The highlighted deck spring elements exhibited the largest deformations during the dynamic analyses. The ductility demand on the brace elements, the storey drift at the building side and at the mid-length were also evaluated.

Development of Hysteretic Model

The objective of the hysteresis study was to select an appropriate rule, as well as to adjust the related parameters, such that the model best replicated the diaphragm behaviour observed in the laboratory. Based on the results of a single quasi-static test by Essa et al. [7] Martin [8] established that the Stewart hysteresis element [13] could be used to model the non-linear / inelastic behaviour of the roof deck diaphragm. However, the short duration loading protocol better represents the earthquake demand when compared to the quasi-static protocol. For this reason it was felt necessary to improve the hysteresis model such that a more accurate prediction of the diaphragm behaviour under seismic loading could be realized. As a basis of comparison nine diaphragm tests, which fall into the three roof type categories (Table 2) were included in the hysteresis study. The selection of parameters for the hysteresis models was based on a comparison of energy values and by inspection of the similarity between the model and the test shear load, S, versus shear deformation, γ, graphs. A selection of these comparisons for the three roof types is shown in Figure 13.

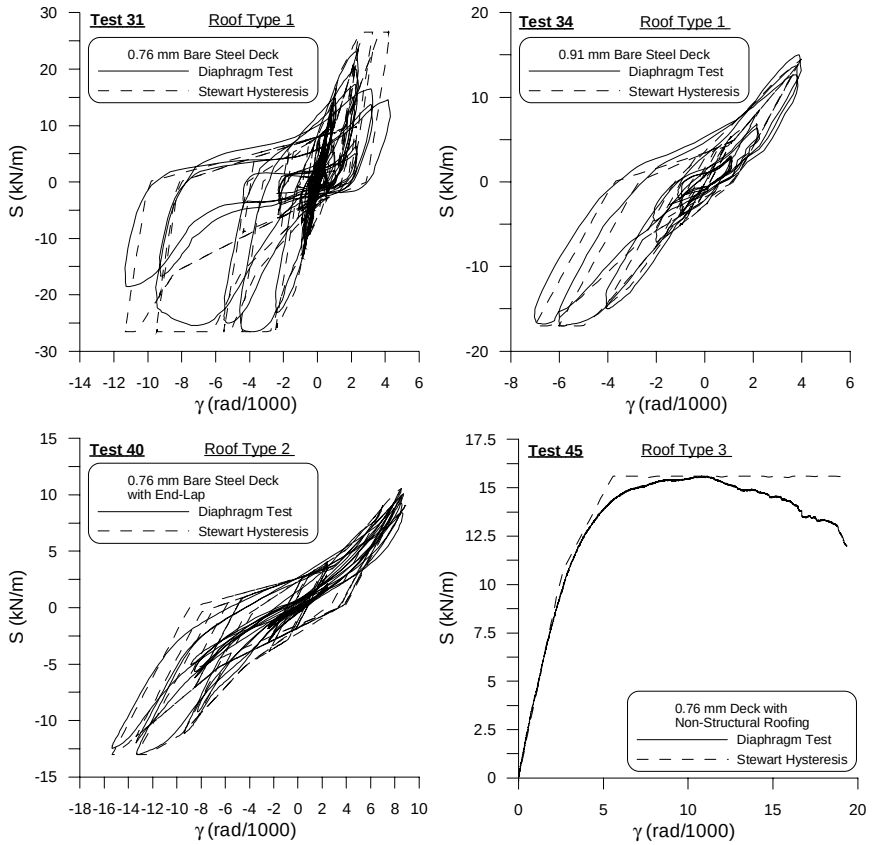

Figure 13 : Comparison of test results with Stewart hysteresis model for roof types 1, 2 and 3

Analysis Results Comparison

Example time history plots of the diaphragm shear distortion, γ, under ground motion 'G' for the three different roof types designed with R_d = 3.0 are provided in Figure 14. These distortions occurred in some of the critical elements near the edges of the diaphragm as highlighted in Figure 6. Lines representing the yield distortion, γ_u, are provided as an indication of which cycles entered into the inelastic range. A comparison of roof type 1 with roof type 2 reveals that the former has a significantly higher diaphragm rigidity, G'=11.9 kN/mm *vs.* 4.31 kN/mm, but they had the same shear capacity S_u=10.1 kN/m. The maximum distortions were 9.85×10^{-3} rad vs. 11.98×10^{-3} rad due to ground motions 'A'; 4.74×10^{-3} rad vs. 7.43×10^{-3} rad due to ground motions 'B'; 11.54×10^{-3} rad vs. 11.34×10^{-3} rad due to ground motions 'G'. Roof type 3 exhibited the smallest shear distortions for all ground motions, which can be attributed to the stiffening and strengthening effect of the non-structural components.

In terms of the R_d = 2.0 buildings, roof types 1 and 2 showed very similar responses since their design properties were almost identical (S_u: 15.3 kN/m vs. 15.4 kN/m; G': 4.57 kN/mm vs. 4.70 kN/mm). The maximum distortions were 9.18 10^{-3} rad vs. 8.77 10^{-3} rad due to ground motions 'A', 4.80×10^{-3} rad vs. 4.30×10^{-3} rad due to ground motions 'B', 5.64×10^{-3} rad vs. 5.19×10^{-3} rad due to ground motions 'G'. Therefore, for the same base shear force, it was possible to design two buildings that behave in a similar fashion even though some parameters were different, e.g. the sheet length. Roof type 3, again because of the roofing materials, displayed a greater stiffness and strength than the other roof types.

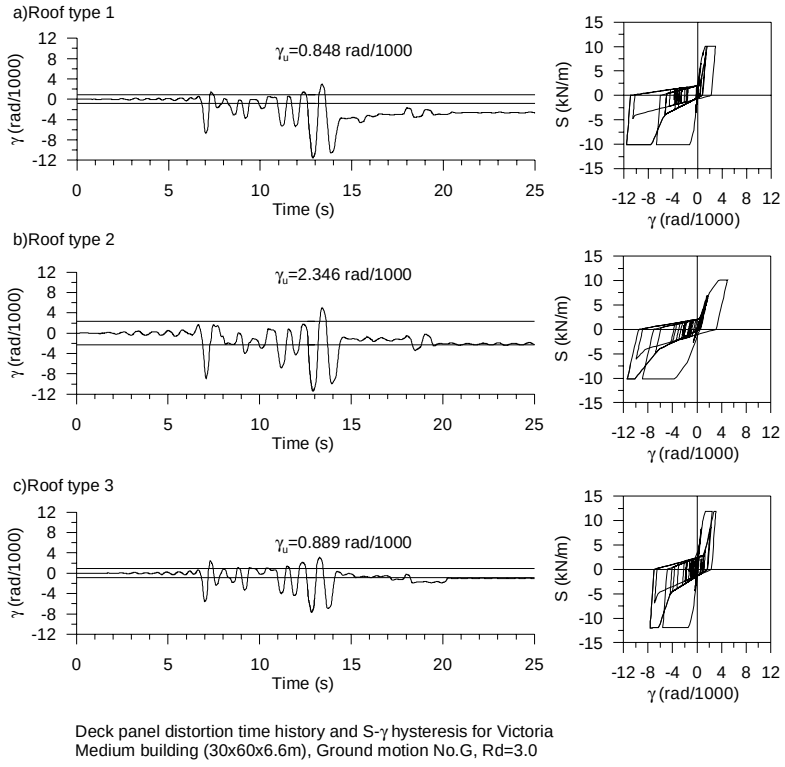

Figure 14 : Time History results for R_d=3.0 and ground motion 'G'

Overall building response

The total deflection at mid-length of the roof, Δ_{total}, including both the lateral movement of the walls and the diaphragm distortion, was used to determine the global ductility demand on the building (Table 3).

This total deflection was compared with the deflection at the point when the shear forces in the diaphragm elements were first equal to S_u of the bare steel design, Δ_y, as follows:

$$\mu_g = \Delta_{total} / \Delta_y \quad (3)$$

Table 3 : Overall building displacements and ductility demand

Analysis Case	R_d=3.0			R_d=2.0		
	Δ_y (mm)	Δ_{total} (mm)	μ_g	Δ_y (mm)	Δ_{total} (mm)	μ_g
1-A		86.4	2.43		124.7	1.66
1-B	35.5	65.3	1.84	75.1	111.9	1.49
1-G		92.8	2.61		108.3	1.44
2-A		124.4	2.26		117.9	1.68
2-B	55.0	89.7	1.63	70.0	101.7	1.45
2-G		121.0	2.20		97.3	1.39
3-A		64.9	2.05		103.0	1.68
3-B	31.6	58.4	1.85	61.3	82.3	1.34
3-G		74.6	2.36		79.0	1.29

Based on the results of the time history analyses the Δ_{total} values in all cases were within the 2.5% inter-storey drift limit of 165 mm. The global ductility demand on the building considering all roof types ranged from 1.63 to 2.61 for R_d = 3.0 and from 1.29 to 1.68 for R_d = 2.0. The end-laps had little effect on the total deflection and global ductility demand for the R_d = 2.0 designed building because the diaphragm stiffness was similar to that for the building with a type 1 roof (Table 2). However, for the R_d = 3.0 building the end-laps resulted in a greater total deflection and slightly less ductility demand because of the more flexible system elastically. The non-structural components caused the total deflection to decrease compared with the type 1 bare steel diaphragm. However, the ductility demand only decreased slightly when the effects of non-structural components were included in the analyses. These analytical findings provide an indication that the trial values of R_d could be used in terms of a global inelastic seismic building response for design.

Local inelastic distortion γ_p and local ductility demand in deck panels μ_D

The inelastic demand was also investigated on a local scale to validate the force modification factors incorporated in the building design. Using the time history analyses the resulting maximum inelastic distortion, γ_p, in the diaphragm was obtained at critical locations (Table 4). The allowable value of $\gamma_p = 10 \times 10^{-3}$ rad defined by Essa *et al.* [7] for nail/screw diaphragm construction was used; which corresponds to the 80% ultimate strength level in the post-peak range. For R_d = 3.0, the inelastic distortions due to ground motions 'A', 'B' and 'G' were all below the allowable limit, except in one case, that is roof type 1 under ground motion 'G'. However, the results are quite variable considering only one building with three earthquake records were utilized. For R_d = 2.0, the γ_p values were all below 10×10^{-3} rad and were also not uniform. A measure of the inelastic deformation in the roof diaphragm can also be made from the local ductility demand, $\mu_D = (\gamma_p + \gamma_u) / \gamma_u$, in the deck panels (Table 5). These localized measures relate the maximum deformation in a specific element with the yield deformation, γ_u. With the R_d = 2.0 designed building the ductility demand values were in the range expected, given the mean value of the different roof types was slightly below 2.0. The R_d = 3.0 building however, experienced a much greater demand in the diaphragm elements than the force modification factor indicates. Tables 4 and 5 also show that end-laps do not have much of an effect on the local inelastic demand, however, the non-structural components can reduce the inelastic distortion for both R_d values.

In a typical structure the local ductility demand can exceed the design R_d value provided that the inelastic demand remains less than the experimental inelastic capacity. Although this was the case for the R_d = 3.0 design, the variability of the γ_p values and their proximity to the experiment based allowable limit, suggest that large inelastic distortions may occur on a local scale in a typical building, possibly causing significant strength degradation. With respect to the non-structural components, even though they seem to reduce the demand on the diaphragm, at this time they should not be relied on in design due to the fact that testing was limited to a single roof system, that variability exists in construction and that a large number of roofing systems with different components are available for use.

Table 4 : Maximum inelastic distortion γ_p (x 10^{-3} rad) in deck panels

R_d value	***R_d=3.0***			***R_d=2.0***		
Roof type	1	2	3	1	2	3
γ_u	0.848	2.346	0.889	3.344	3.269	2.817
Ground motion						
A	9.01	9.64	4.99	5.84	5.50	3.64
B	3.89	5.09	2.80	1.46	1.03	0.68
G	10.70	9.00	6.77	2.30	1.93	0.80
Mean	7.87	7.91	4.85	3.20	2.82	1.71
Maximum	10.70	9.64	6.77	5.84	5.50	3.64

Table 5 : Ductility demand μ_D in deck panels

R_d value	***R_d=3.0***			***R_d=2.0***		
Roof type	1	2	3	1	2	3
Ground motion						
A	11.63	5.11	6.61	2.75	2.68	2.29
B	5.59	3.17	4.15	1.44	1.32	1.24
G	13.62	4.84	8.62	1.69	1.59	1.28
Mean	10.28	4.37	6.46	1.96	1.86	1.61
Maximum	13.62	5.11	8.62	2.75	2.68	2.29

CONCLUSIONS

A summary of experimental and analytical findings from the most recent study in a research project covering the seismic design of single-storey steel buildings and their diaphragms was presented. The design of these buildings is based on the assumption that the steel roof deck diaphragm will act as the energy-dissipating element in the seismic force resisting system. This paper detailed the effect of non-structural components and the presence of end-lap joints / panel length on diaphragm performance. Large-scale diaphragm tests revealed that the presence of non-structural roofing components, such as gypsum and fibre board, caused the in-plane diaphragm stiffness and strength to increase by 49% and 24%, respectively. Furthermore, the use of shorter length deck sections with end-lap connections resulted in an overall reduction in the diaphragm stiffness and strength because of increased panel warping effects. Also included were the results of non-linear time history dynamic building analyses, which accounted for the variation in behaviour due to the non-structural roof components, the use of end-laps and the short duration seismic loading behaviour. These analyses showed that the end-laps did not have a significant effect on the inelastic demand placed on the diaphragm, whereas the non-structural components contributed to a reduction in demand. Global ductility demand on the building was in the range of the R_d values used for design, while local ductility demand in the diaphragm was variable with the highest values near the inelastic limit ($\gamma_p = 10 \times 10^{-3}$ rad) based on previous experimental results. Much greater

variability and higher local ductility values were obtained for the R_d = 3.0 designed building. At this stage, it is recommended that a force modification factor R_d not greater than 2.0 be used in the case where the diaphragm is expected to experience inelastic demand in the SFRS. In addition, the non-structural roofing components should not be relied on the reduce the inelastic demand on the diaphragm due to the large number of roofing systems with different components that are available, because only two tests were carried out on one type of roofing system, and because variability exists in construction.

ACKNOWLEDGEMENTS

The authors would like to acknowledge the support provided by the Natural Sciences and Engineering Research Council of Canada, the Steel Structures Education Foundation (Canadian Institute of Steel Construction), the Canam Manac Group, the Canadian Sheet Steel Building Institute, the Canadian Welding Bureau, the Steel Deck Institute, Hilti Corp., and ITW Buildex Inc.. A thank you is also extended to G. Degrange, D. Fortier and P. Bélanger of the Structural Engineering Laboratory at École Polytechnique of Montreal, and the undergraduate students who assisted with the testing.

REFERENCES

1. Canadian Standards Association S16. "Limit States Design of Steel Structures". Mississauga, Canada, 2001.
2. National Research Council of Canada, Institute for Research In Construction. "Proposed changes to NBC 1995 – Part 4". Ottawa, Canada, 2001.
3. Steel Deck Institute. "Diaphragm Design Manual". Canton, USA, 1981.
4. Steel Deck Institute. "Diaphragm Design Manual". Second Edition. Canton, USA, 1991.
5. Davies, J.M., Bryan, E.R.. "Manual of Stressed Skin Diaphragm Design". John Wiley and Sons Inc., New York, USA, 1982.
6. Tremblay, R., Rogers, C.A., Martin, E., Yang, W.. "Analysis, Testing and Design of Steel Roof Deck Diaphragms for Ductile Earthquake Resistance", *Journal of Earthquake Engineering*, In Press.
7. Essa, H.S., Tremblay, R., Rogers, C.A.. "Behavior of Roof Deck Diaphragms Under QuasiStatic Cyclic Loading", *Journal of Structural Engineering, ASCE*, Vol. 129 No. 12, 1658-1666, 2003.
8. Martin, E.. "Inelastic Response of Steel Roof Deck Diaphragms Under Simulated Dynamically Applied Seismic Loading". Masters Thesis, Dept. of Civil, Geological and Mining Engineering, Ecole Polytechnique, Montreal, Canada, 2002.
9. Yang, W.. "Inelastic Seismic Response of Steel Roof Deck Diaphragms Including Effects of Non-Structural Components and End Laps". Masters Thesis, Dept. of Civil, Geological and Mining Engineering, Ecole Polytechnique, Montreal, Canada, 2003.
10. American Society for Testing and Materials A653. "Standard Specification for Steel Sheet, Zinc-Coated (Galvanized) or Zinc-Iron Alloy-Coated (Galvannealed) by the Hot-Dip Process", West Conshohocken, USA, 2002.
11. Mitchell, D., Tremblay, R., Karacabeyli, E., Paultre, P., Saatcioglu, M., Anderson, D.. "Seismic force modification factors for the proposed 2005 edition of the National Building Code of Canada". *Can. J. Civ. Eng*. 30: 308-327. 2003.
12. Carr, A.J.. "RUAUMOKO – Inelastic Dynamic Analysis". Version March 15th 2000. Dept. of Civil Eng., University of Canterbury, Christchurch, New Zealand. 2000.
13. Stewart, W.G.. "The Seismic Design of Plywood Sheathed Shear Walls". Ph.D. Thesis, Department of Civil Engineering, University of Canterbury, Christchurch, New Zealand, 1987.